

Document downloaded from:

<http://hdl.handle.net/10251/80987>

This paper must be cited as:

Desantes Fernández, JM.; Bermúdez, V.; López, JJ.; López Pintor, D. (2016). A new method to predict high and low-temperature ignition delays under transient thermodynamic conditions and its experimental validation using a Rapid Compression-Expansion Machine. *Energy Conversion and Management*. 123:512-522. doi:10.1016/j.enconman.2016.06.051.



The final publication is available at

<http://dx.doi.org/10.1016/j.enconman.2016.06.051>

Copyright Elsevier

Additional Information

A new method to predict high and low-temperature ignition delays under transient thermodynamic conditions and its experimental validation using a Rapid Compression-Expansion Machine

José M. Desantes^a, Vicente Bermúdez^a, J. Javier López^{a,*}, Darío López-Pintor^a

^a*CMT-Motores Térmicos
Universitat Politècnica de València
Camino de Vera, s/n. 46022 Valencia, SPAIN*

Abstract

A new procedure to predict both high-temperature stage and cool flames ignition delays under transient thermodynamic conditions has been developed in this paper. The results obtained have been compared with those obtained from the Livengood & Wu integral method, as well as with other predictive methods and with direct chemical kinetic simulations and experimental data. All simulations have been performed with CHEMKIN, employing a detailed chemical kinetic mechanism. The simulations and predictions have been validated in the working range versus experimental results obtained from a Rapid Compression-Expansion Machine (RCEM). The study has been carried out with n-heptane and iso-octane, as diesel and gasoline fuel surrogates, under a wide range of initial temperatures (from $358K$ to $458K$), initial pressures ($0.14MPa$ and $0.17MPa$), compression ratios (15 and 17), EGR rates (from

*Corresponding author
Tel: +34 963 879 232. Fax: +34 963 877 659. E-mail: jolosan3@mot.upv.es

0% to 50%) and equivalence ratios (from 0.3 to 0.8). The experimental results show good agreement with the direct chemical kinetic simulations and with the new predictive method proposed. In fact, the mean relative deviation between experiments and simulations is equal to 1.719% for n-heptane and equal to 1.504% for iso-octane. Besides, the new method has shown good predictive capability not only for the high-temperature stage of the process but also for cool flames, being the mean relative deviation versus the experimental data lower than 2.900%. Better predictions of the ignition delay have been obtained with the new procedure than the ones obtained with the classic Livengood & Wu expression, especially in those cases showing a two-stage ignition pattern.

Keywords: RCEM, ignition delay, autoignition modeling, fuels, chemical processes

1. Introduction, justification and objective

Advanced combustion modes based on the autoignition of a premixed mixture with a certain degree of homogeneity, such as Homogeneous Charge Compression Ignition (HCCI), Premixed Charge Compression Ignition (PCCI), Reactivity Controlled Compression Ignition (RCCI) and others, have been studied for the simultaneous reduction of soot and NO_x [1]. Their working principle is based on Low Temperature Combustion (LTC) by avoiding the soot and NO_x formation peninsulas, which can be seen in equivalence ratio - temperature diagrams [2] and their effectiveness has been widely proved in previous studies [3, 4]. These modes show virtually zero emissions of soot and NO_x , but high emissions of unburned hydrocarbons (UHC) and

12 carbon monoxide (CO) that can be easily eliminated with well-known after-
13 treatment techniques. The lack of control over the autoignition process and
14 over the heat release rate are the main challenge to implement these new com-
15 bustion strategies in commercial reciprocating internal combustion engines
16 [5].

17 Ignition is controlled by the chemical kinetics of the charge in these new
18 combustion modes [6]. This control entails higher complexity because of the
19 absence of an explicit ignition-controlling event, such as a spark or an in-
20 jection process when very reactive conditions are reached in the combustion
21 chamber (near top dead center). The reactivity of the mixture can be modi-
22 fied by adjusting the engine operating parameters, such as the Exhaust Gas
23 Recirculation (EGR) rate and the inlet temperature. Therefore, improving
24 the capability of predicting the autoignition is mandatory to properly modify
25 the operating conditions of the engine and to control the heat release.

26 The autoignition event can be reasonably well predicted by using ad-
27 vanced CFD codes with detailed chemistry. However, the required comput-
28 ing time is too long to be solved in real time. Simple numerical methods
29 with very short computing time are the only ones that can be implemented
30 in an engine control unit. If these low computing time methods have enough
31 accuracy to properly predict ignition delays, the control of the engine can be
32 improved since decisions in real time can be taken.

33 Moreover, the use of detailed chemical kinetic mechanisms coupled with
34 CFD codes is limited by the physical discretization of the domain. The com-
35 putational cost of solving detailed chemistry in cases with a high number of
36 cells could be unacceptable, imposing the use of simplified mechanisms. The

37 total computing time can be reduced by implementing predictive numeri-
38 cal methods to determine the ignition delay instead of solving the involved
39 reaction rates.

40 The Livengood & Wu hypothesis [7], also known as the Livengood & Wu
41 integral method, allows to obtain ignition delays of processes under transient
42 conditions of temperature and pressure by using the ignition characteristics
43 under constant thermodynamic conditions, which are much easier to obtain
44 both experimentally and by simulation. The expression proposed by these
45 authors is the following:

$$\int_0^{t_i} \frac{1}{\tau} dt = 1 \quad (1)$$

46 where t_i is the ignition delay of the process and τ is the ignition delay under
47 constant conditions of pressure and temperature for the successive thermo-
48 dynamic states.

49 The Livengood & Wu integral assumes that the autoignition happens
50 when a critical concentration of chain carriers is reached, being this critical
51 concentration constant with pressure and temperature for a given air-fuel
52 mixture. Besides, the oxidation process during the ignition delay is described
53 by a single zero-order global reaction and, therefore, the reaction rate does
54 not depend on time under constant thermodynamic conditions. The negative
55 temperature coefficient (NTC) behavior cannot be correctly modeled under
56 these hypotheses.

57 This integral has been traditionally enunciated as a method to predict
58 knock in SI-engines [8]. However, it has been extended to CI-engines as a
59 way to predict the ignition delay of homogeneous air-fuel mixtures as the

60 ones used in HCCI combustion modes [9]. Several authors such as Ohyama
61 [10], Rausen et al. [11], Choi et al. [12] and Hillion et al. [13] studied the
62 implementation of the Livengood & Wu integral in an engine control unit.
63 These authors used the integral method to predict the start of combustion
64 under HCCI conditions. This method can be combined with other simple
65 models to obtain global parameters of the combustion process allowing the
66 control of the engine in real time.

67 The integral method has been used in several CFD studies as the model
68 to predict the autoignition delay. For example, Imamori et al. [14] coupled
69 the Livengood & Wu integral with Star-CD and KIVA 3 to improve the
70 performance of a low speed two-stroke diesel engine. And Li et al. [15]
71 linked the integral method with the CFD code VECTIS to study the effects
72 of heterogeneities on a two-stroke HCCI engine fueled with gasoline.

73 The validity of the Livengood & Wu integral when a two-stage ignition
74 occurs has been wondered by several authors [16]. The integral method
75 is not able to accurately predict the ignition delay because it is based on
76 a single global reaction mechanism that ignores the cool flames. Some of
77 these authors, as Liang and Reitz [17] or Edenhofer et al. [18], show the
78 need to create simple algorithms, but more sophisticated than the integral
79 method, to characterize the autoignition at low temperatures without using
80 any chemical kinetic mechanism, since the integral method has great interest
81 for the prediction of autoignition due to its simplicity and low computational
82 cost. However, few alternatives to the Livengood & Wu integral can be found
83 in the literature.

84 Hernandez et al. [19] analyzed the validity of the Livengood & Wu in-

85 tegral by simulations performed with CHEMKIN for several fuels and with
86 various chemical kinetics mechanisms. They proved that the predictions of
87 the method are accurate if the fuel do not show a two-stage ignition pat-
88 tern. These authors also proposed two different alternatives, one with better
89 and another with worse results than the integral method. However, most of
90 the alternatives proposed to improve the integral method are based on the
91 method itself or assume the same hypotheses, which are too simplified.

92 Desantes et al. [20, 21] have proposed two different methods based on the
93 Glassman’s model to predict ignition delays referred to a critical concentra-
94 tion of chain carriers, which are previous works related to the current one.
95 The hypothesis of constant critical concentration is avoided in both methods,
96 whereas one of them also avoids the description of the autoignition process
97 by a single zero-order global reaction. However, since the ignition delay is
98 defined as the time when a critical concentration of chain carriers is reached,
99 only ignition delays referred to critical concentrations can be predicted ac-
100 curately. Therefore, the high exothermic phase of the ignition cannot be
101 obtained, since the critical concentration occurs in a previous stage, as will
102 be shown later in section 2.

103 Numerical expressions based on more sophisticated autoignition models
104 are needed in order to extend the range of validity of the methods. Moreover,
105 both exothermic stages should be predicted in the case of fuels that show two-
106 stage ignition: cool flames and high-exothermic heat release. The validity
107 of a possible procedure to determine both ignition delays under transient
108 conditions is intended to be solved in this work. The study has been done
109 with n-heptane and iso-octane, the reactivities of which are very similar to

110 diesel fuel and gasoline, respectively. Despite the fact that more sophisticated
111 surrogate fuels for diesel can be found in the literature, n-heptane and iso-
112 octane were chosen because extended and fully validated chemical kinetic
113 mechanisms are available for both. Moreover, they are primary reference
114 fuels (PRFs) employed to define the octane number reference scale, and they
115 are widely used in the literature as diesel fuel and gasoline surrogates under
116 engine conditions [22].

117 Simulations have been performed with the software of chemical simulation
118 CHEMKIN. This software, which is developed by Reaction Design (ANSYS),
119 is consolidated in the world of engineering investigations, and the chemical
120 kinetics mechanisms of several hydrocarbons are perfectly defined to be used
121 with it. Finally, the numerical results are validated experimentally using a
122 Rapid Compression-Expansion Machine (RCEM).

123 The structure of the paper is the following: first, the theoretical develop-
124 ment of a new expression to predict ignition delays under transient conditions
125 is explained. Then, the experimental facilities involved in the study are pre-
126 sented. Afterwards, the methodological approach is described, including the
127 experimental methods, the chemical kinetic simulations and the parametric
128 study performed. Thereafter, the new method is validated with the experi-
129 mental results and its predictive ability is compared with the chemical kinetic
130 simulations and with other predictive methods. Finally, the conclusions of
131 this study are shown.

132 **2. Theoretical development of a new predictive method for ignition**
133 **delays**

134 A new method to predict the ignition delay under transient thermody-
135 namic conditions is obtained starting from the integral method proposed by
136 Desantes et al. [21]. This new procedure intends to be able to predict not
137 only the ignition delay referred to cool flames but also the ignition delay
138 referred to the high-temperature exothermic stage of the process. Models
139 based on a critical concentration of chain carriers are not able to accurately
140 predict exothermic stages, since the critical concentration of chain carriers
141 is reached before the sudden heat release rate. Thus, alternative procedures
142 should be proposed, since exothermic stages are the only ones that can be
143 easily measured experimentally.

144 In this section, two different theoretical developments are described. On
145 the one hand, a predictive method for cool flames is explained. This method
146 is based on the accumulation of chain carriers up to reach a maximum of
147 concentration, which should occur at the same time than cool flames. HO_2
148 is selected as chain carrier since it seems to be a good tracer of such phe-
149 nomenon. Thus, $CC = \text{HO}_2$, where CC represents the chain carriers. On
150 the other hand, a complementary predictive method for the high-temperature
151 stage of the combustion process is developed. This method is based on the
152 consumption of chain carriers from the critical concentration, therefore, it is
153 a consecutive method to the one used for the accumulation of chain carriers.
154 The selected chain carrier should be completely consumed when the sudden
155 heat release occurs. Thus, $CC = \text{CH}_2\text{O}$ for this second method. Three
156 different ignition delays are defined in the following paragraphs:

- 157 • τ_1 is the ignition delay under constant thermodynamic conditions re-
158 ferred to the maximum pressure rise caused by cool flames.
- 159 • τ_2 is the ignition delay under constant thermodynamic conditions re-
160 ferred to the maximum pressure rise caused by the high-temperature
161 stage of the combustion process.
- 162 • τ_{CC} is the ignition delay under constant thermodynamic conditions
163 referred to the critical concentration of chain carriers. Different species
164 are proposed as chain carrier depending on the stage of the ignition
165 to be predicted: $CC = HO_2$ for cool flames and $CC = CH_2O$ for the
166 high-temperature stage of the process.

167 *2.1. Prediction of cool flames*

168 As it is explained in detail in [21], assuming that during the ignition
169 delay the termination reactions are not very important, since $[O_2] \gg [CC]$
170 and $[F] \gg [CC]$ (where F represents the fuel), and considering an air-fuel
171 mixture under constant conditions of temperature and pressure, the following
172 expression for the evolution of the concentration of chain carriers can be
173 obtained:

$$[CC] = [CC]_{max} \frac{t}{\tau_{CC}} \quad (2)$$

174 where $[CC]_{max}$ represents the critical concentration of chain carriers (maxi-
175 mum concentration of chain carriers, which defines the ignition time).

176 If a process under transient conditions of pressure and temperature is
177 discretized as a series of thermodynamic states that remain constant for a

178 time dt , the ignition time referred to a critical concentration of chain carriers
 179 can be obtained as follows:

$$1 = \frac{1}{[CC]_{max,t_i,CC}} \int_0^{t_{i,CC}} \frac{[CC]_{max}}{\tau_{CC}} dt \quad (3)$$

180 where $t_{i,CC}$ is the ignition delay of the process referred to a maximum concen-
 181 tration of chain carriers and τ_{CC} and $[CC]_{max}$ are the ignition delay referred
 182 to a maximum of chain carriers and the critical concentration of chain carri-
 183 ers, respectively, under constant conditions of pressure and temperature for
 184 the successive thermodynamic states.

185 The theoretical development for the obtention of Eq. 3 is described in
 186 detail in [21]. It should be noted that if the critical concentration of chain
 187 carriers is considered as a constant, Eq. 3 results in the Livengood & Wu
 188 integral.

189 Despite the fact that Eq. 3 represents a method to predict ignition delays,
 190 only times of ignition referred to a critical concentration of chain carriers can
 191 be obtained. Therefore, the high exothermic stage of the process cannot be
 192 predicted, since the maximum heat release rate occurs always after reaching
 193 the critical concentration of chain carriers. However, as can be seen in Fig. 1,
 194 a maximum in concentration of HO_2 is reached at the same time where the
 195 maximum pressure rise rate of cool flames occurs. Therefore, the cool flames
 196 time can be predicted by taking into account HO_2 as chain carrier and HO_2
 197 was selected as a good tracer of this phenomenon.

198 Finally, a schematic of Eq. 3 can be seen in Fig. 1. The accumulation
 199 behavior of HO_2 is modeled by the accumulated area of Eq. 3, by using the
 200 τ_{CC} and $[CC]_{max}$ functions related with this species. Once the value of 1

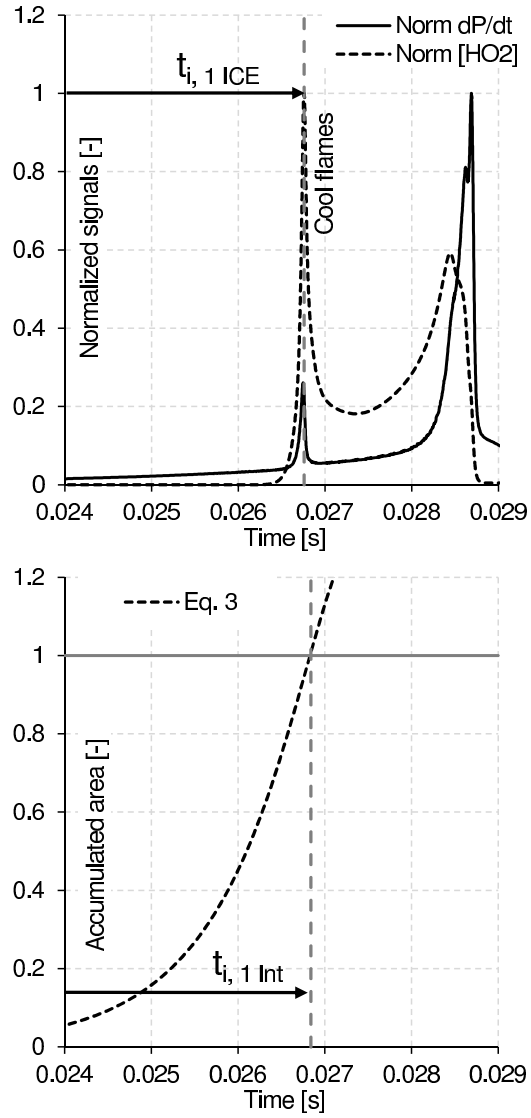


Figure 1: Accumulated area of Eq. 3 compared to normalized concentration of HO_2 and normalized pressure rise rate, both obtained from CHEMKIN for $T_i=408\text{ K}$, $P_i=0.14\text{ MPa}$, $CR=15$, $X_{O_2}=0.147$, $Fr=0.4$, n-heptane.

201 is reached, the time at which the maximum concentration of HO₂ occurs is
 202 predicted and, therefore, the ignition delay referred to cool flames is obtained.

203 *2.2. Prediction of the high-temperature stage*

204 The maximum heat release rate occurs when all the chain carriers are
 205 consumed. From a theoretical point of view, the heat release can be assumed
 206 as a sudden event. Therefore, considering an air-fuel mixture under constant
 207 thermodynamic conditions, the temperature and pressure conditions from
 208 the maximum concentration of chain carriers up to their disappearance can
 209 be assumed as invariants. Thus, and as it is explained in more detail in Ap-
 210 pendix A, the evolution of the consumption of chain carriers can be obtained
 211 as:

$$[CC] = [CC]_{max} \frac{\tau_2 - t}{\tau_2 - \tau_{CC}} \quad (4)$$

212 where τ_2 represents the ignition delay referred to the maximum heat release
 213 rate.

214 Discretizing the process under transient conditions of pressure and tem-
 215 perature in a series of thermodynamic states that remain constant for a time
 216 dt , the ignition time referred to the high exothermic stage of the combustion
 217 can be obtained as follows:

$$1 = \frac{1}{[CC]_{max,t_i,CC}} \int_{t_i,CC}^{t_{i,2}} \frac{[CC]_{max}}{\tau_2 - \tau_{CC}} dt \quad (5)$$

218 where τ_{CC} , τ_2 and $[CC]_{max}$ are respectively the ignition delay referred to a
 219 maximum of chain carriers, the ignition delay referred to the high exothermic

220 stage and the critical concentration of chain carriers under constant condi-
221 tions of pressure and temperature for the successive thermodynamic states.

222 A schematic of this new procedure is shown in Fig. 2. CH_2O is selected
223 as chain carrier, since formaldehyde is widely recognized as an autoignition
224 tracer [23]. The time at which the maximum concentration of CH_2O is
225 reached can be predicted by using Eq. 3, which accumulated area represents
226 the accumulation behavior of this chain carrier. Then, the consumption
227 of CH_2O is modeled by the accumulated area of Eq. 5, by using the τ_{CC}
228 and $[CC]_{max}$ functions related with this species. It should be noted that
229 the decomposition of chain carriers starts once the value of 1 is reached in
230 Eq. 3 (once the maximum concentration of chain carriers is reached). When
231 the accumulated area of Eq. 5 is equal to 1, the time at which all CH_2O
232 is consumed is predicted and, therefore, the ignition delay referred to the
233 high-temperature stage is obtained.

234 The combination of Eq. 3 and Eq. 5 allows the prediction of the time of
235 ignition referred to a maximum heat release rate (or pressure rise rate) under
236 variable thermodynamic conditions, which is a parameter easily measurable
237 in experimental facilities. It should be noted that if the fuel does not present
238 a two-stage ignition, τ_{CC} and τ_2 are virtually the same, and the ignition
239 delays predicted for both integrals, $t_{i,CC}$ and $t_{i,2}$, are also virtually the same.
240 A more detailed explanation about this theoretical development can be found
241 in Appendix A.

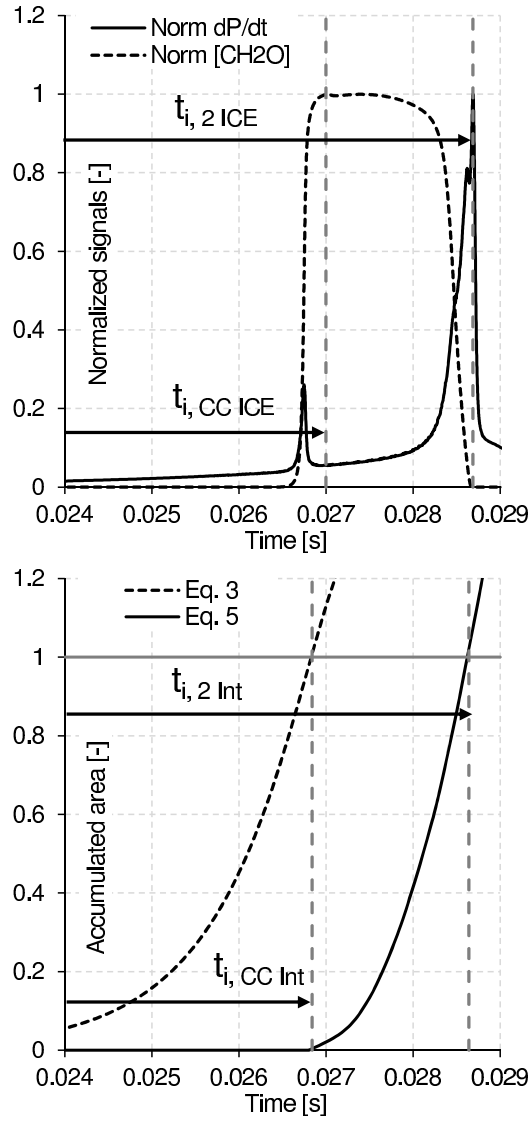


Figure 2: Accumulated area of Eq. 3 and Eq. 5 compared to the concentration of chain carriers (CH_2O) and the pressure rise rate. $T_i=408\text{ K}$, $P_i=0.14\text{ MPa}$, $CR=15$, $X_{O_2}=0.147$, $Fr=0.4$, n-heptane.

242 **3. Materials and methods**

243 The accuracy of the new method to predict ignition delays was analyzed
244 by comparison with the results of a parametric study performed in a RCEM
245 following this methodology: for a certain case, the evolutions of both the
246 in-cylinder temperature and pressure are experimentally obtained under mo-
247 toring conditions. Then, the ignition delay, τ , and the critical concentration,
248 $[CC]_{max}$, are obtained for each thermodynamic state by simulation in a per-
249 fectly stirred reactor. The ignition delay under transient conditions is then
250 predicted by using the new procedure proposed in this paper and the Liven-
251 good & Wu integral method. Besides, the ignition delay under transient
252 conditions is obtained experimentally and it is also calculated by simulat-
253 ing it in an internal combustion engine reactor (direct chemical simulation)
254 solving the detailed chemical kinetics mechanism. Finally, the predicted ig-
255 nition delays and the values obtained from the direct chemical simulations
256 are compared directly with the experimental results.

257 *3.1. RCEM*

258 A RCEM is an experimental facility widely used in autoignition studies
259 due to its capability to reproduce engine conditions [24]. It can replicate
260 reasonably well the combustion process of reciprocating engines with fully
261 controlled initial and boundary conditions and avoiding the complexities as-
262 sociated to engines [25].

263 Different compression ratios can be reached in the RCEM by varying the
264 stroke and the clearance volume. An axial optical access is available [26]
265 and the compression velocity can be varied in order to simulate the effect of

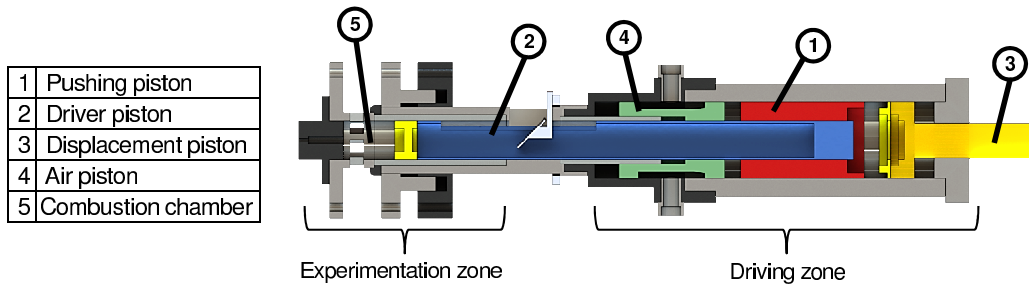


Figure 3: Rapid Compression Expansion Machine schematic.

266 different engine speeds. In a RCEM, part of the expansion stroke of the piston
 267 can be also analyzed, and most of the engine parameters can be calculated,
 268 such as the heat release rate or the combustion efficiency. In this facility both
 269 homogeneous and heterogeneous (direct injection) mixtures can be tested, as
 270 well as new combustion modes such as the dual fuel technology [27] or LTC
 271 [28].

272 A schematic of the RCEM is shown in Figure 3. The RCEM is pneu-
 273 matically driven and its pistons are hydraulically coupled. The machine can
 274 be divided in two different zones: the experimentation zone and the driving
 275 zone. The experimentation zone is composed by the combustion chamber,
 276 while the driving zone is composed by four different pistons. Piston 1 (push-
 277 ing piston) is pneumatically driven and hydraulically coupled to piston 2
 278 (driver piston), which is directly connected with the combustion chamber.
 279 Piston 3 is hydraulically driven and it can be adjusted to select the com-
 280 pression stroke. Finally, piston 4 contains the compressed air that drives the
 281 machine. Further details on the operation principle of the RCEM can be
 282 found in [29].

Bore	84	mm
Stroke	120 - 249	mm
Compression ratio	5 - 30	-
Maximum cylinder pressure	200	bar
Initial pressure	1 - 5	bar
Maximum heating temperature	473	K

Table 1: Technical characteristics of the RCEM.

283 The technical characteristics of the RCEM can be seen in Table 1. The
 284 pushing piston and the driver piston are instrumented with two AMO LMK102
 285 incremental position sensors (0.01mm of resolution), which allow knowing
 286 the absolute position of each piston and, therefore, the combustion chamber
 287 volume. The combustion chamber is composed by three elements: the ex-
 288 perimentation piston (mechanically connected to the driver piston), the liner
 289 and the cylinder head. The experimentation piston consists of a steel-made
 290 piston with a 84mm bore and a quartz-made bowl with cylindrical shape,
 291 50mm of bore and 2.2mm in depth, which allows the axial optical access.
 292 As the bowl is flat, the chamber images can be recorded without any image
 293 distortion.

294 Besides, the cylinder head and the cylinder liner have different heating
 295 elements arranged in six separately controlled zones, which are responsible
 296 for heating the cylinder walls and the experimentation piston. The wall tem-
 297 perature is measured by a total of six K-type thermocouples, two located in
 298 the cylinder head and four in the liner. Very good temperature homogeneity
 299 has been observed [29], with a standard deviation in gas temperature of the

300 order of $3K$. It was found that the distribution of temperature is barely
301 affected by the gas in-flow due to its low speed. An initial gas temperature
302 equal to the wall temperature is achieved due to the long duration of the
303 intake process.

304 The cylinder head is instrumented with a Kistler 7061B cooled piezoelec-
305 tric pressure sensor ($-80pC/bar$ of sensitivity), which is coupled to a Kistler
306 5011 charge amplifier, and whereby the in-cylinder pressure is measured.
307 Different piezo-resistive pressure sensors are available to control the filling of
308 the driving gas and of the combustion chamber ($0.01bar$ of resolution). The
309 injection system is composed by a Siemens hollow cone piezo-injector with
310 a cone angle of 90° , which is centered in the cylinder head. Its fuel delivery
311 rate has been previously measured with an IAV injection rate analyzer. The
312 transient signals have been recorder at $100kHz$ with a PC-based transient
313 measurement recorder. The RCEM is filled from an external tank that can
314 be heated up to $373K$. The synthetic air is produced in the tank by a filling
315 based on partial pressures where N_2 , CO_2 and O_2 can be used. The mixture
316 is analyzed in a Horiba PG-250 portable gas analyzer in order to know the
317 exact composition and ensure the correct reproduction of the experiments in
318 CHEMKIN.

319 The desired stroke of the machine is selected and the RCEM is heated up
320 to the desired temperature. The synthetic air-EGR mixture is prepared in
321 the mixing tank by a filling based on partial pressures. In this study, EGR
322 was considered as the products of a complete combustion reaction between
323 the fuel and dry air in which the amount of oxygen is the one desired by
324 the user, as explained in [30]. The combustion chamber is scavenged several

325 times before the filling. The fuel is injected into the combustion chamber
326 at the start of the intake process to avoid problems of stratification or other
327 inhomogeneities. The long duration of the process (approximately 40s), is
328 enough to guarantee a homogeneous environment in the chamber when the
329 compression stroke starts.

330 In order to ensure a representative ignition delay time measurement, the
331 number of repetitions of each point has been selected so that the semi-
332 amplitude of the confidence interval with a level of confidence of 95% is
333 smaller than 1% of the mean ignition delay value.

334 In this work the autoignition of the mixture is considered to be produced
335 when the time derivative of the pressure signal (which will be referred as
336 pressure rise rate further on) reaches a maximum. Thus, the ignition delay
337 in the experimental facility is defined as the time between the start of the
338 rapid compression process, which is a constant reference due to constructive
339 aspects of the machine, and the instant in which the maximum pressure
340 rise is obtained, as can be seen in Fig. 4. This way, cool flames and high
341 temperature ignition delay can be easily distinguished in case of having two-
342 stage ignition.

343 Finally, the temperature profile is calculated for each experiment by ap-
344 plying the energy equation, since the pressure profile and the position of the
345 piston are known. The heat losses are characterized by a model based on the
346 Woschni correlation [31]. The calculation includes two additional models for
347 deformations and leaks, both of them explained in [32, 33].

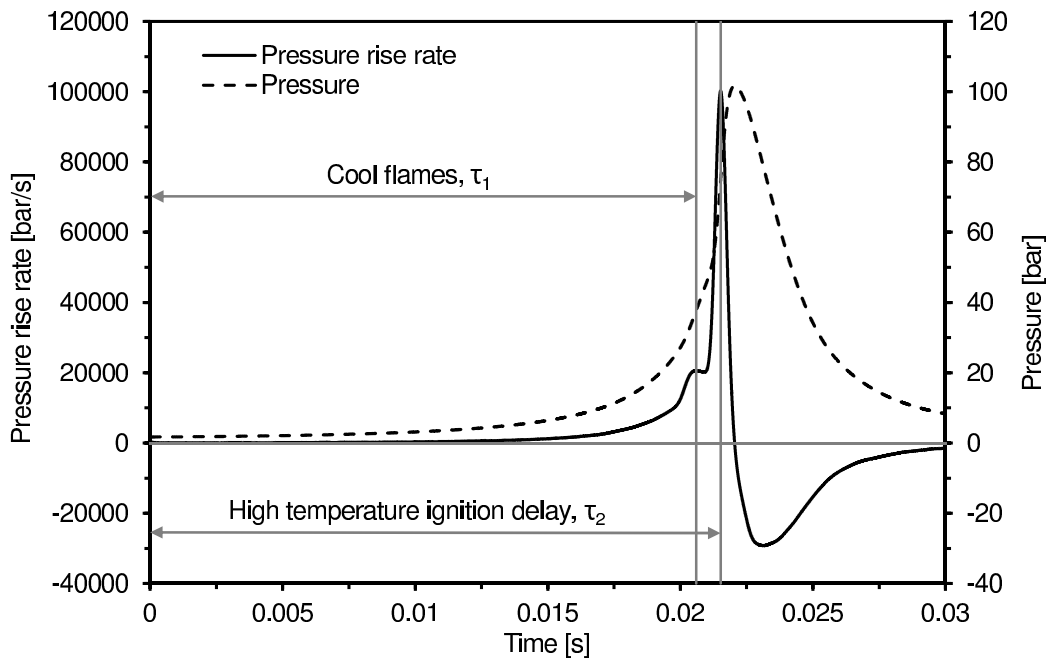


Figure 4: Ignition delay definition. The autoignition of the mixture is considered to be produced when the maximum pressure rise occurs.

348 *3.2. CHEMKIN and chemical kinetic mechanisms*

349 CHEMKIN-PRO is the software used to obtain the different ignition de-
350 lays and critical concentrations. The Curran's kinetic mechanism is used for
351 *n*-heptane and *iso*-octane [34, 35]. This mechanism consists of 1034 species
352 and 4238 reactions, and includes the chemical kinetics of the two hydro-
353 carbons used in this investigation. Its validity has been checked in several
354 articles [22, 36] by comparison with experimental results.

355 The model used to obtain ignition delays under constant conditions, τ_{CC} ,
356 τ_1 and τ_2 , and critical concentrations is a homogeneous closed reactor (per-
357 fectly stirred reactor, PSR), which works with constant pressure and uses the
358 energy equation to solve the temperature temporal evolution. This model is
359 the most appropriate to obtain ignition delays at constant pressure and tem-
360 perature conditions [37].

361 The model used to obtain ignition delays under transient conditions is a
362 reciprocating internal combustion engine operating with homogeneous charge
363 (IC-engine, closed 0-D reactors from CHEMKIN). The volume profile as well
364 as the heat loss profile are imposed in order to reproduce the RCEM condi-
365 tions. The piston starts at bottom dead center (BDC) and a complete cycle
366 of the RCEM is simulated. The autoignition is considered to be produced
367 when the time derivative of the pressure signal reaches a maximum. This is
368 the same criterion than the used in the experiments and, therefore, it allows
369 comparing the simulated results directly with the experimental ones.

370 Finally, the ignition delays and the critical concentration are obtained
371 for each thermodynamic state with a Δt of $10^{-5}s$, which is the experimental
372 resolution of the pressure signal. This value of the time step also represents

373 an equilibrium between appropriate prediction accuracy and reasonable cal-
374 culation time. Besides, the maximum waiting time for the autoignition of
375 the mixture has been set to 30 s.

376 3.3. Parametric study performed

377 The performed experimental study was as follows:

- 378 • Fuel: *n*-heptane and *iso*-octane.
- 379 • Initial temperature (T_i): 358K (only for n-heptane), 383K, 408K,
380 433K and 458K.
- 381 • Initial pressure (P_i): 0.14MPa and 0.17MPa.
- 382 • Compression stroke: 249mm.
- 383 • Compression ratio (CR): 15 and 17.
- 384 • Oxygen molar fraction (X_{O_2}): 0.21 (0% EGR), 0.147 (30% EGR), 0.126
385 (40% EGR) and 0.105 (50% EGR).
- 386 • Equivalence ratio (Fr): from 0.3 to 0.8 depending on the fuel and on
387 the oxygen mass fraction.

388 The maximum equivalence ratio is limited by the working oxygen molar
389 fraction in order to avoid extremely violent combustions. The equivalence
390 ratio of 0.4 has been chosen as base point in order to have the possibility to
391 try leaner and richer mixtures without damaging the facility. The performed
392 parametric study can be seen in Table 2. Finally, the temperature of the
393 combustion chamber is always above the boiling point of the fuel, therefore
394 ensuring that the fuel is in vapor phase before the beginning of the cycle.

		T_i [K]				
		358	383	408	433	458
Fr [-]	0.3	<i>40</i>		0, 30, 40, 50		40
	0.4	<i>0, 30, 40, 50</i>	40, 50	0, 30, 40, 50	40, 50	0, 30, 40, 50
	0.5	<i>40</i>	40	40, 50	40	40
	0.6	<i>40</i>		40, 50		40
	0.7			40, 50		
	0.8			40, 50		

Table 2: Parametric study performed. EGR percent for different initial temperatures and equivalence ratios. *Italic.-* exclusively for n-heptane. **Bold.-** exclusively for iso-octane.

395 4. Validation and results

396 Ignition delays obtained solving the n-heptane and iso-octane detailed
397 chemical kinetic mechanism are compared with the experimental results as
398 a method to validate the mechanism in the desired range. Moreover, the
399 experimental ignition delay is intended to be predicted by using not only the
400 integral method presented in this paper (Eq. 3 and 5) but also the Livengood
401 & Wu integral method. Two different events have been studied from a point
402 of view of the auto-ignition process: cool flames and the high exothermic stage
403 of the ignition process.

404 4.1. Predictive methods applied to cool flames

405 Cool flames is a phenomenon only present in the cases performed with
406 n-heptane. Ignition delays referred to cool flames are obtained experimen-
407 tally and by direct chemical kinetic simulation in CHEMKIN. Besides, two
408 different predictive methods have been evaluated. First, the integral method

409 described by Eq. 3 has been used assuming HO_2 as chain carrier. It is not
 410 necessary to evaluate Eq. 5, since no disappearance of chain carriers occurs
 411 at the same instant than cool flames. Finally, the Livengood & Wu inte-
 412 gral method (Eq. 1) has been applied by using a τ_1 function referred to cool
 413 flames.

414 The percentage deviation in ignition delay, ϵ , was calculated in order to
 415 compare more easily experimental and simulation results. This deviation is
 416 defined as follows:

$$\epsilon = \frac{t_{i,1x} - t_{i,1RCEM}}{t_{i,1RCEM}} 100 \quad (6)$$

417 where $t_{i,1}$ represents the time of ignition (ignition delay under transient con-
 418 ditions) referred to cool flames. The subscript x can represent either data
 419 obtained from a chemical simulation with CHEMKIN using a closed 0-D
 420 IC-engine reactor, *ICE*, from the new predictive method, *Int*, or from the
 421 Livengood & Wu integral method, *LW*. Finally, the subscript *RCEM* rep-
 422 resents data obtained experimentally from the RCEM.

423 The ignition delay deviations between the chemical kinetic simulations
 424 and the experimental results are shown in Fig. 5 for all cases that show
 425 a two-stage ignition pattern. The mean absolute deviation, $|\bar{\epsilon}|$, has been
 426 calculated and its value can be seen in the figure.

427 The results show that simulations are able to reproduce the experimental
 428 ignition delays with quite good accuracy. In fact, the confidence interval for
 429 the mean absolute deviation, $|\bar{\epsilon}|$, with a confidence level of 95% is equal to
 430 [1.331, 4.345]. Ignition delay deviations are caused partly by the chemical
 431 kinetic mechanism used and partly by the uncertainties in the calculation of

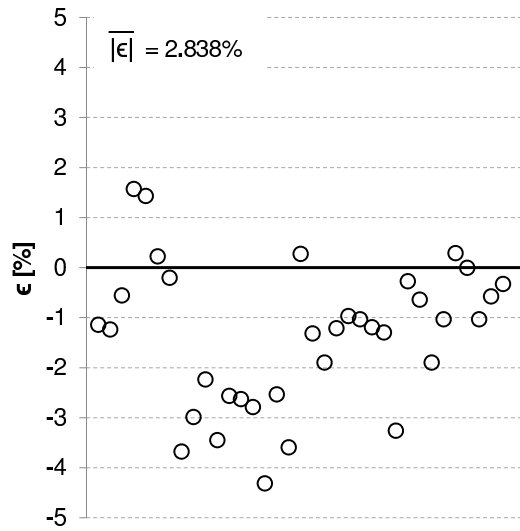


Figure 5: Percentage deviation in ignition delay. The mean absolute deviation, $|\bar{\epsilon}|$, shows good agreement between both experimental and simulated results.

432 the effective volume and the heat losses of the RCEM. It can be seen that the
 433 ignition delay referred to cool flames is underestimated by the mechanism. As
 434 Fig. 6 shows, this is mainly caused because of the higher pressure rise rate
 435 calculated by CHEMKIN. Despite the fact that cool flames start in both
 436 cases approximately at the same instant, the maximum pressure rise rate is
 437 reached much faster in the simulations, which leads to a certain deviation
 438 between these cases and the experiments. The absence of wall effects and
 439 heterogeneities in CHEMKIN causes a faster pressure rise not only in the
 440 case of cool flames, but also in the case of the high-temperature stage of the
 441 process.

442 The predicted ignition delays also show quite good agreement with the
 443 experimental results. The confidence intervals for $|\bar{\epsilon}|$ with a confidence level

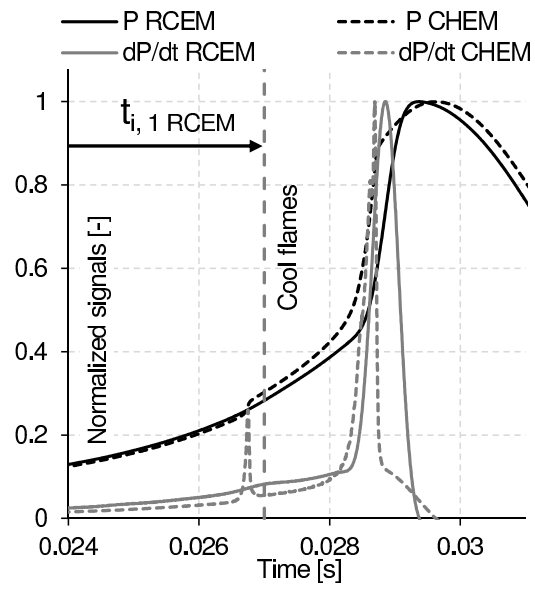


Figure 6: Pressure signal and pressure rise rate obtained experimentally and by simulation.
 $T_i=408\text{ K}$, $P_i=0.14\text{ MPa}$, $CR=15$, $X_{O_2}=0.147$, $Fr=0.4$, n-heptane.

444 of 95% are summarized in Table 3 for the predictive methods. These values
 445 of $|\bar{\epsilon}|$ are very similar to each other, meaning that both predictive methods
 446 are able to predict the ignition delay referred to cool flames with the same
 447 accuracy than the detailed chemical kinetic mechanism.

	n-Heptane
CHEMKIN	[1.331, 4.345]%
New integral proposed	[1.064, 4.204]%
Livengood & Wu	[1.066, 4.155]%

Table 3: Confidence interval for the mean absolute deviation referred to cool flames, $|\bar{\epsilon}|$, with a confidence level of 95% for the chemical kinetic simulations (CHEMKIN) and for the different predictive methods.

448 HO_2 can be assumed as a good tracer of cool flames, since the time of
 449 ignition referred to a critical concentration of HO_2 predicted by Eq. 3 shows
 450 good agreement with the time of ignition of cool flames. Moreover, it should
 451 be noted that the Livengood & Wu integral method can be used to predict
 452 cool flames without assuming high deviations.

453 4.2. Predictive methods applied to the high exothermic stage

454 Ignition delays referred to a maximum pressure rise rate are obtained
 455 experimentally and by direct chemical kinetic simulations in CHEMKIN.
 456 Moreover, three different predictive methods have been evaluated now:

- 457 • The integral method described by Eq. 3 and Eq. 5 has been used,
 458 assuming CH_2O as a chain carrier.
- 459 • The Livengood & Wu integral method (Eq. 1) has been applied by
 460 using a τ_2 function referred to a maximum pressure rise.

461 • The alternative integral proposed by Hernandez et al. [19] has also
462 been evaluated for the cases that show cool flames.

463 This last alternative method consists of solving the following two integrals:

$$1 = \int_0^{t_{i,1}} \frac{1}{\tau_1} dt \quad (7)$$

$$1 = \int_{t_{i,1}}^{t_{i,2}} \frac{1}{\tau_2 - \tau_1} dt \quad (8)$$

464 where $t_{i,1}$ and τ_1 represents ignition delays referred to cool flames and $t_{i,2}$
465 and τ_2 represents ignition delays referred to the maximum pressure rise rate.
466 Obviously, it is not possible to use this method with fuels that show a single-
467 stage ignition, and therefore it has been evaluated only for n-heptane.

468 It should be noted that the new method proposed in this paper (Eq. 3 and
469 5) is a general method that can be used for all fuels, since the ignition delay
470 referred to a critical concentration of chain carriers can be defined despite
471 the absence of cool flames.

472 The percentage deviation in ignition delay, ϵ , was calculated in order to
473 compare more easily experimental and simulation results. This deviation is
474 defined as follows:

$$\epsilon = \frac{t_{i,2x} - t_{i,2RCEM}}{t_{i,2RCEM}} 100 \quad (9)$$

475 where $t_{i,2}$ represents the time of ignition (ignition delay under transient con-
476 ditions) referred to a maximum pressure rise rate. The subscript x can repre-
477 sent either data obtained from a chemical simulation with CHEMKIN using

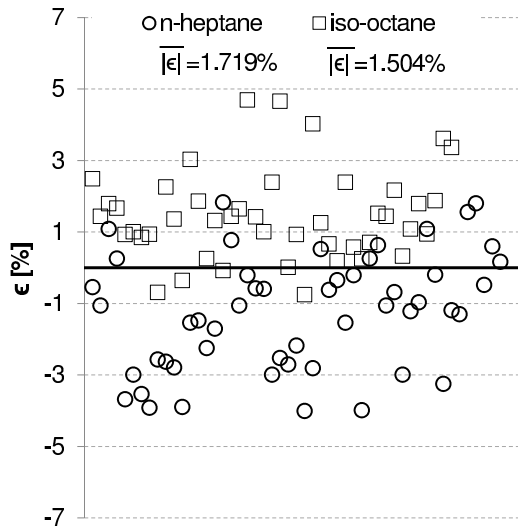


Figure 7: Percentage deviation in ignition delay. The mean absolute deviation, $|\bar{\epsilon}|$, shows a good agreement between both experimental and simulated results.

478 a closed 0-D IC-engine reactor, *ICE*, from the new predictive method, *Int*,
 479 from the Livengood & Wu integral method, *LW*, or from the alternative
 480 method proposed by Hernandez, *LW – mod*. Finally, the subscript *RCEM*
 481 represents data obtained experimentally from the RCEM.

482 The ignition delay deviations between the chemical kinetic simulations
 483 and the experimental results are shown in Fig. 7 for all cases. The mean
 484 absolute deviation, $|\bar{\epsilon}|$, has been calculated and its value can be seen in the
 485 figure.

486 The results show that simulations are able to reproduce the experimental
 487 ignition delays with quite good accuracy. In fact, the confidence interval
 488 for the mean absolute deviation, $|\bar{\epsilon}|$, with a confidence level of 95% is equal
 489 to [1.331, 1.984] for n-heptane and equal to [1.213, 1.894] for iso-octane. As

490 before, ignition delay deviations are caused partly by the chemical kinetic
491 mechanism used and partly by the uncertainties in the calculation of the
492 effective volume and the heat losses in the RCEM. It can be seen that the
493 ignition delay referred to a maximum pressure rise is underestimated for n-
494 heptane but overestimated for iso-octane. As explained in [24], this fact is
495 probably because the rates of alkyl-peroxy radical isomerization and peroxy-
496 alkylhydroperoxy radical isomerization have been decreased by a factor of
497 three compared to n-heptane in the case of the iso-octane sub-mechanism.

498 The confidence intervals for $|\bar{\epsilon}|$ with a confidence level of 95% are summa-
499 rized in Table 4 for all the predictive methods. The new integral method pro-
500 posed in this paper shows good agreement with the experiments. However,
501 the accuracy of the Livengood & Wu integral method shows a strong depen-
502 dence on the type of fuel. It can be seen that the Livengood & Wu integral
503 is able to predict accurately the ignition delay referred to the high exother-
504 mic stage of combustion if the fuel shows a single-stage ignition (iso-octane),
505 but the predictive capability is significantly reduced when a two-stage igni-
506 tion occurs (n-heptane). Finally, the method proposed by Hernandez et al.
507 shows poor predictive capability, but better results than the Livengood &
508 Wu integral.

509 The Livengood & Wu predictive method assumes that autoignition oc-
510 curs when a critical concentration of chain carriers is reached. Therefore, only
511 ignition delays referred to a critical concentration can be predicted, which oc-
512 cur at a different stage than the maximum pressure rise rate. Moreover, only
513 information referred to a critical concentration of chain carriers, τ , should
514 be used in the integral by definition of the method itself. These facts cause

	n-Heptane	iso-Octane
CHEMKIN	[1.331, 1.984]%	[1.213, 1.894]%
New integral proposed	[1.751, 3.686]%	[0.907, 1.817]%
Livengood & Wu	[5.894, 14.354]%	[0.898, 1.855]%
Hernandez et al.	[5.623, 11.778]%	-

Table 4: Confidence interval for the mean absolute deviation referred to a maximum pressure rise, $|\bar{\epsilon}|$, with a confidence level of 95% for the chemical kinetic simulations (CHEMKIN) and for the different predictive methods.

515 an intrinsic deviation between predictions and experimental results, which
516 leads to unacceptable predictions for fuels that show cool flames. It should
517 be noted that if the fuel does not present a two-stage ignition pattern or if
518 it presents a very smooth (or inexistent) NTC zone, the different ignition
519 delays are virtually the same and the Livengood & Wu integral method can
520 predict ignition delays with high accuracy.

521 5. Conclusions

522 In this work a new method to predict ignition delays under transient
523 conditions from those obtained under constant conditions is developed. The
524 method allows to obtain not only the ignition delay referred to cool flames but
525 also the time of ignition referred to a critical concentration of chain carriers
526 and referred to a maximum pressure rise rate. Finally, this new method
527 shows better results than the Livengood & Wu integral method.

528 A detailed chemical kinetic mechanism has been validated in the working
529 range versus experimental results obtained from a RCEM. Besides, the new

530 predictive method and the Livengood & Wu integral have also been compared
531 to the experiments.

532 The following conclusions can be deduced from this study:

- 533 • Cool flames can be accurately reproduced with all the predictive meth-
534 ods used in this paper, since the critical concentration of HO_2 occurs
535 at the same instant than the maximum pressure rise associated to this
536 phenomenon. Thus, HO_2 can be assumed as a cool flames tracer.

- 537 • The new integral method proposed by the authors has shown a good
538 predictive capability related with ignition delays referred to a maximum
539 pressure rise rate. Therefore, the predicted ignition delays can be easily
540 measured experimentally. Moreover, the new integral method does not
541 depend on the existence of cool flames, since it can be applied for all
542 type of fuels.

- 543 • The Livengood & Wu integral method is able to predict ignition de-
544 lays referred to the high exothermic stage of combustion only if the
545 fuel shows a single-stage ignition. This method is originally based on
546 the premise that autoignition occurs when the critical concentration
547 of chain carriers is reached. Therefore, the predicted ignition delays
548 will be referred to this criterion and the information used to obtain
549 the predictions may be also referred to this criterion. Otherwise, an
550 intrinsic deviation between predictions obtained from the Livengood &
551 Wu integral and the experimental results appears, since both ignition
552 delays could be referred to different stages of the combustion process. If
553 the fuel does not present a two-stage combustion or if the NTC zone is

554 very soft, all criteria to define the ignition delay are virtually the same
555 and they can be compared with each other. Thus, the Livengood &
556 Wu integral can be used with high accuracy to predict ignition delays
557 of single-stage ignition fuels but not with fuels that show a two-stage
558 ignition pattern.

559 **Acknowledgements**

560 The authors would like to thank different members of the CMT-Motores
561 Térmicos team of the Universitat Politècnica de València for their contri-
562 bution to this work. The authors would also like to thank the director of
563 LAV-ETH, Konstantinos Boulouchos, for the Darío López-Pintor’s intern-
564 ship at LAV. Finally, the authors would like to thank the Spanish Ministry
565 of Education for financing the PhD. Studies of Darío López-Pintor (grant
566 FPU13/02329).

567 **Notation**

<i>BDC</i>	Bottom Dead Center
<i>CC</i>	Chain carriers
<i>CFD</i>	Computational Fluid Dynamics
<i>CI</i>	Compression Ignition
<i>CR</i>	Compression Ratio
<i>EGR</i>	Exhaust Gas Recirculation
568 <i>Fr</i>	Working equivalence ratio
<i>HCCI</i>	Homogeneous Charge Compression Ignition
<i>ICE</i>	Referred to data obtained from CHEMKIN using the internal combustion engine reactor
<i>Int</i>	Referred to data obtained from the new integral proposed in this paper

<i>LW</i>	Referred to data obtained from the Livengood & Wu integral method
<i>LW – mod</i>	Referred to data obtained from the predictive method proposed by Hernandez et al. [19]
<i>LTC</i>	Low Temperature Combustion
<i>max</i>	Referred to a maximum concentration of chain carriers
<i>NTC</i>	Negative Temperature Coefficient
P_i	Initial pressure
<i>PCCI</i>	Premixed Charge Compression Ignition
<i>PRF</i>	Primary Reference Fuels
<i>PSR</i>	Perfectly Stirred Reactor
⁵⁶⁹ <i>RCCI</i>	Reactivity Controlled Compression Ignition
<i>RCEM</i>	Rapid Compression-Expansion Machine
<i>SI</i>	Spark Ignition
T_i	Initial temperature
<i>TDC</i>	Top Dead Center
t_i	Ignition delay under transient conditions
$t_{i,CC}$	Ignition delay referred to the critical concentration of chain carriers
$t_{i,1}$	Ignition delay referred to the maximum pressure rise of cool flames
$t_{i,2}$	Ignition delay referred to the maximum pressure rise
<i>UHC</i>	Unburned hydrocarbons

X_{O_2}	Oxygen molar fraction
ϵ	Percentage deviation in ignition delay between experimental and simulation or predicted results
$ \bar{\epsilon} $	Mean absolute deviation between experimental and simulation or predicted results
τ	Ignition delay under constant conditions of pressure and temperature
⁵⁷⁰ τ_{CC}	Ignition delay under constant thermodynamic conditions referred to the critical concentration of chain carriers
τ_1	Ignition delay under constant thermodynamic conditions referred to the maximum pressure rise of cool flames
τ_2	Ignition delay under constant thermodynamic conditions referred to the maximum pressure rise

⁵⁷¹ **Appendix A. Theoretical development of a new expression to pre-**
⁵⁷² **dict high-temperature ignition delays**

⁵⁷³ Ignition delays referred to a maximum pressure rise occur after the crit-
⁵⁷⁴ ical concentration of chain carriers is reached, once all chain carriers have
⁵⁷⁵ disappeared. Besides, the accumulative behavior of the chain carriers and
⁵⁷⁶ the time at which this critical concentration is reached can be predicted for
⁵⁷⁷ a certain evolution of pressure and temperature by the following equation
⁵⁷⁸ developed by Desantes et al. [21]:

$$1 = \frac{1}{[CC]_{max,t_{i,CC}}} \int_0^{t_{i,CC}} \frac{[CC]_{max}}{\tau_{CC}} dt \quad (\text{A.1})$$

579 where $t_{i,CC}$ is the ignition delay of the process referred to a maximum concen-
580 tration of chain carriers, and τ_{CC} and $[CC]_{max}$ are the ignition delay referred
581 to a maximum of chain carriers and the critical concentration of chain carri-
582 ers, respectively, under constant conditions of pressure and temperature for
583 the successive thermodynamic states.

584 Therefore, it is possible to study the decomposition of chain carriers from
585 $t_{i,CC}$ and, thus, to obtain the ignition delay under transient thermodynamic
586 conditions referred to the maximum pressure rise rate, $t_{i,2}$.

587 Starting from the Glassman's model for autoignition [38], the global dis-
588 appearance rate of chain carriers, $[CC]$, can be written as:

$$\frac{d[CC]}{dt} = k_1[R] + ((k_2(\alpha - 1) - k_4) [R] - k_5) [CC] \quad (\text{A.2})$$

589 where $[R]$ represents the fuel, α is a multiplicative factor that represents the
590 chain behavior of $[CC]$ and k_1 , k_2 , k_4 and k_5 represent the specific reac-
591 tion rate of the initiation reaction, the chain reaction, the main termination
592 reaction and the termination reaction by wall effects, respectively.

593 Taking into account that the termination reactions are dominant after
594 reaching the critical concentration of chain carriers, the previous equation
595 can be written as:

$$\frac{d[CC]}{dt} = -(k_4[R] + k_5) [CC] = -A[CC] \quad (\text{A.3})$$

596 where A depends on specific reaction rates and on the fuel concentration.

597 Assuming a process under constant conditions of pressure and temper-
598 ature during the ignition delay, and assuming that $[R] \gg [CC]$, Eq. A.3
599 can be integrated with the condition $[CC] = [CC]_{max}$ when $t = \tau_{CC}$ (ig-
600 nition delay under constant thermodynamic conditions referred to a critical
601 concentration) as follows:

$$\frac{[CC]}{[CC]_{max}} = \exp(A(\tau_{CC} - t)) \quad (\text{A.4})$$

602 The exponential term in Eq. A.4 can be approximated by a Taylor series
603 expansion that can be truncated in the second term, resulting in the following
604 expression:

$$\frac{[CC]}{[CC]_{max}} = 1 + A(\tau_{CC} - t) \quad (\text{A.5})$$

605 taking into account the condition $[CC] = 0$ when $t = \tau_2$ (ignition delay
606 under constant thermodynamic conditions referred to a maximum pressure
607 rise), the following expression can be finally obtained for the evolution of chain
608 carriers:

$$\frac{[CC]}{[CC]_{max}} = \frac{\tau_2 - t}{\tau_2 - \tau_{CC}} \quad (\text{A.6})$$

609 equation that is only valid under constant conditions of pressure and tem-
610 perature, since otherwise Eq. A.3 cannot be integrated.

611 If a process under transient thermodynamic conditions is discretized as
612 a series of thermodynamic states that remain constant for a time dt , the
613 ignition time can be obtained by discretizing Eq. A.6 as follows:

$$\frac{d[CC]}{[CC]_{max}} = -\frac{dt}{\tau_2 - \tau_{CC}} \quad (\text{A.7})$$

614 and integrating it during the period of time between the critical concentration
 615 of chain carriers and the maximum heat release rate:

$$\int_{[CC]_{max,t_i,CC}}^0 d[CC] = - \int_{t_i,CC}^{t_{i,2}} \frac{[CC]_{max}}{\tau_2 - \tau_{CC}} dt \rightarrow 1 = \frac{1}{[CC]_{max,t_i,CC}} \int_{t_i,CC}^{t_{i,2}} \frac{[CC]_{max}}{\tau_2 - \tau_{CC}} dt \quad (\text{A.8})$$

616 where $t_{i,2}$ is the ignition delay of the process referred to a maximum heat
 617 release rate, and τ_{CC} , τ_2 and $[CC]_{max}$ are the ignition delay referred to a
 618 maximum of chain carriers, the ignition delay referred to the high exothermic
 619 stage and the critical concentration of chain carriers under constant condi-
 620 tions of pressure and temperature for the successive thermodynamic states,
 621 respectively.

622 It should be noted that Eq. A.8 can be combined with Eq. A.1 to predict
 623 both ignition delays referred to a critical concentration and, starting from it,
 624 the one referred to a maximum pressure rise rate.

625 References

- 626 [1] J. Benajes, S. Molina, A. García, and J. Monsalve-Serrano. Effects of
 627 direct injection timing and blending ratio on RCCI combustion with dif-
 628 ferent low reactivity fuels. *Energy Conversion and Management*, 99:193–
 629 209, 2015.

- 630 [2] Z. Zheng, L. Yue, H. Liu, Y. Zhu, X. Zhong, and M-Yao. Effect of
631 two-stage injection on combustion and emissions under high EGR rate
632 on a diesel engine by fueling blends of diesel/gasoline, diesel/n-butanol,
633 diesel/gasoline/n-butanol and pure diesel. *Energy Conversion and Man-*
634 *agement*, 90:1–11, 2015.
- 635 [3] T. Li, D. Wu, and M. Xu. Thermodynamic analysis of EGR effects on
636 the first and second law efficiencies of a boosted spark-ignited direct-
637 injection gasoline engine. *Energy Conversion and Management*, 70:130–
638 138, 2013.
- 639 [4] J. Benajes, J.V. Pastor, A. García, and J. Monsalve-Serrano. An exper-
640 imental investigation on the influence of piston bowl geometry on RCCI
641 performance and emissions in a heavy-duty engine. *Energy Conversion*
642 *and Management*, 103:1019–1030, 2015.
- 643 [5] S.S. Nathan, J.M. Mallikarjuna, and A. Ramesh. An experimental study
644 of the biogas-diesel HCCI mode of engine operation. *Energy Conversion*
645 *and Management*, 51:1347–1353, 2010.
- 646 [6] K. Bahlouli, U. Atikol, R.K. Saray, and V. Mohammadi. A reduced
647 mechanism for predicting the ignition timing of a fuel blend of natural-
648 gas and n-heptane in HCCI engine. *Energy Conversion and Manage-*
649 *ment*, 79:85–96, 2014.
- 650 [7] J.C. Livengood and P.C. Wu. Correlation of autoignition phenomena in
651 internal combustion engines and rapid compression machines. *Sympo-*
652 *sium (International) on Combustion*, 5:347–356, 1955.

- 653 [8] L. Chen, T. Li, T. Yin, and B. Zheng. A predictive model for knock
654 onset in spark-ignition engines with cooled EGR. *Energy Conversion*
655 *and Management*, 87:946–955, 2014.
- 656 [9] M. Shahbakhti, R. Lupul, and C. R. Koch. Predicting HCCI auto-
657 ignition timing by extending a modified knock-integral method. *SAE*
658 *Paper no. 2007-01-0222*, 2007.
- 659 [10] Y. Ohyama. Engine control using a combustion model. *Seoul 2000*
660 *FISITA World Automotive Congress*, 2000.
- 661 [11] D.J. Rausen, A.G. Stefanopoulou, J.M. Kang, J.A. Eng, and T.W. Kuo.
662 A mean-value model for control of homogeneous charge compression
663 ignition HCCI engines. *Journal of Dynamic Systems, Measurement,*
664 *and Control*, 127:355–362, 2005.
- 665 [12] Y. Choi and J.Y. Chen. Fast prediction of start-of-combustion in HCCI
666 with combined artificial neural networks and ignition delay model. *Pro-*
667 *ceedings of the Combustion Institute*, 30:2711–2718, 2005.
- 668 [13] M. Hillion, J. Chauvin, and N. Petit. Control of highly diluted com-
669 bustion in diesel engines. *Control Engineering Practice*, 19:1274–1286,
670 2011.
- 671 [14] Y. Imamori, H. Endo, K. Sakaguchi, and J. Yanagi. Development of
672 combustion system in low speed two-stroke diesel engine using CFD.
673 *International Council on Combustion Engines*, 2004.
- 674 [15] G. Li, T. Bo, C. Chen, and R.J.R. Johns. CFD simulation of HCCI

- 675 combustion in a 2-stroke DI gasoline engine. *SAE Paper no. 2003-01-*
676 *1855*, 2003.
- 677 [16] A.D.B. Yates, A. Swarts, and C.L. Viljoen. Correlating auto-ignition
678 delays and knock-limited spark-advance data for different types of fuel.
679 *SAE Paper no. 2005-01-2083*, 2005.
- 680 [17] L. Liang and R.D. Reitz. Spark ignition engine combustion modeling
681 using a level set method with detailed chemistry. *SAE Paper no. 2006-*
682 *01-0243*, 2006.
- 683 [18] R. Edenhofer, K. Lucka, and H. Kohne. Low temperature oxidation of
684 diesel-air mixtures at atmospheric pressure. *Proceedings of the Combustion*
685 *Institute*, 31:2947–2954, 2007.
- 686 [19] J.J. Hernandez, M. Lapuerta, and J. Sanz-Argent. Autoignition pre-
687 diction capability of the Livengood-Wu correlation applied to fuels of
688 commercial interest. *International Journal of Engine Research*, 15:817–
689 829, 2014.
- 690 [20] J. M. Desantes, J. J. López, S. Molina, and D. López-Pintor. Validity
691 of the Livengood & Wu correlation and theoretical development of an
692 alternative procedure to predict ignition delays under variable thermo-
693 dynamic conditions. *Energy Conversion and Management*, 105:836–847,
694 2015.
- 695 [21] J. M. Desantes, J. J. López, S. Molina, and D. López-Pintor. Theo-
696 retical development of a new procedure to predict ignition delays un-
697 der transient thermodynamic conditions and validation using a Rapid

- 698 Compression-Expansion Machine. *Energy Conversion and Management*,
699 108:132–143, 2016.
- 700 [22] M. Sjoberg and J.E. Dec. An investigation into lowest acceptable com-
701 bustion temperatures for hydrocarbon fuel in HCCI engines. *Proceedings*
702 *of the Combustion Institute*, 30:2719–2726, 2005.
- 703 [23] B. Baeuerle, J. Warnatz, and F. Behrendt. Time-resolved investigation
704 of hot spots in the end gas of an S.I. engine by means of 2-D double-
705 pulse LIF of formaldehyde. *Symposium (International) on Combustion*,
706 2:2619–26256, 1996.
- 707 [24] J. M. Desantes, J.M. García-Oliver, W. Vera-Tudela, D. López-Pintor,
708 B. Schneider, and K. Boulouchos. Study of ignition delay time and
709 generalization of auto-ignition for PRFs in a RCEM by means of natural
710 chemiluminescence. *Energy Conversion and Management*, 111:217–228,
711 2016.
- 712 [25] G. Barroso, A. Escher, and K. Boulouchos. Experimental and numerical
713 investigations on HCCI combustion. *SAE Paper no. 2005-24-038*, 2005.
- 714 [26] D. Mitakos, C. Blomberg, A. Vandersickel, Y. Wright, B. Schneider,
715 and K. Boulouchos. Ignition delays of different homogeneous fuel-air
716 mixtures in a Rapid Compression Expansion Machine and comparison
717 with a 3-stage-ignition model parametrized on shock tube data. *SAE*
718 *Paper no. 2013-01-2625*, 2013.
- 719 [27] S. Schlatter, B. Schneider, Y. Wright, and K. Boulouchos. Compara-
720 tive study of ignition systems for lean burn gas engines in an optically

- 721 accessible Rapid Compression Expansion Machine. *SAE Paper no. 2013-*
722 *24-0112*, 2013.
- 723 [28] T. Steinhilber and T. Sattelmayer. The effect of water addition on HCCI
724 diesel combustion. *SAE Paper no. 2006-01-3321*, 2006.
- 725 [29] S. Schlatter, B. Schneider, Y. Wright, and K. Boulouchos. Experimental
726 study of ignition and combustion characteristics of a diesel pilot spray
727 in a lean premixed methane/air charge using a Rapid Compression Ex-
728 pansion Machine. *SAE Paper no. 2012-01-0825*, 2012.
- 729 [30] J. M. Desantes, J. J. López, S. Molina, and D. López-Pintor. Design
730 of synthetic EGR and simulation study of the effect of simplified for-
731 mulations on the ignition delay of isooctane and n-heptane. *Energy*
732 *Conversion and Management*, 96:521–531, 2015.
- 733 [31] G. Woschni. A universally applicable equation for the instantaneous
734 heat transfer coefficient in the internal combustion engine. *SAE Paper*
735 *no. 670931*, 1967.
- 736 [32] J. Benajes, P. Olmeda, J. Martín, and R. Carreño. A new methodology
737 for uncertainties characterization in combustion diagnosis and thermo-
738 dynamic modelling. *Applied Thermal Engineering*, 71:389–399, 2014.
- 739 [33] F. Payri, S. Molina, J. Martín, and O. Armas. Influence of measure-
740 ment errors and estimated parameters on combustion diagnosis. *Applied*
741 *Thermal Engineering*, 26:226–236, 2006.

- 742 [34] H.J. Curran, P. Gaffuri, Pitz W.J, and C.K. Westbrook. A comprehen-
743 sive modeling study of n-heptane oxidation. *Combustion and Flame*,
744 114:149–177, 1998.
- 745 [35] H.J. Curran, P. Gaffuri, Pitz W.J, and C.K. Westbrook. A comprehen-
746 sive modeling study of iso-octane oxidation. *Combustion and Flame*,
747 129:253–280, 2002.
- 748 [36] H.J. Curran, W.J. Pitz, C.K. Westbrook, C.V. Callahan, and F.L. Dryer.
749 Oxidation of automotive primary reference fuels at elevated pressures.
750 *Proceedings of the Combustion Institute*, 27:379–387, 1998.
- 751 [37] F. Payri, X. Margot, S. Patouna, F. Ravet, and M. Funk. Use of a
752 single-zone thermodynamic model with detailed chemistry to study a
753 natural gas fueled Homogeneous Charge Compression Ignition engine.
754 *Energy Conversion and Management*, 53:298–304, 2012.
- 755 [38] I. Glassman and R.A. Yetter. *Combustion*. Elsevier Academic Press,
756 2008.